Universal Spreading of Wave Packets in Disordered Nonlinear Systems

S. Flach, D. O. Krimer, and Ch. Skokos

Max Planck Institute for the Physics of Complex Systems, Nöthnitzer Strasse 38, D-01187 Dresden, Germany

In the absence of nonlinearity all eigenmodes of a chain with disorder are spatially localized (Anderson localization). The width of the eigenvalue spectrum and the average eigenvalue spacing inside the localization volume set two frequency scales. An initially localized wave packet spreads in the presence of nonlinearity. Nonlinearity introduces frequency shifts, which define three different evolution outcomes: (i) localization as a transient, with subsequent subdiffusion; (ii) the absence of the transient and immediate subdiffusion; (iii) self-trapping of a part of the packet and subdiffusion of the remainder. The subdiffusive spreading is due to a finite number of packet modes being resonant. This number does not change on average and depends only on the disorder strength. Spreading is due to corresponding weak chaos inside the packet, which slowly heats the cold exterior. The second moment of the packet grows as t^α. We find $\alpha = \frac{1}{3}$.

The normal modes (NMs) of a one-dimensional linear system with uncorrelated random potential are spatially localized (Anderson localization). Therefore any wave packet, which is initially localized, remains localized for all time [1]. When nonlinearities are added, NMs interact with each other [2]. Recently, experiments were performed on light propagation in spatially random nonlinear optical media [3] and on Bose-Einstein condensate expansions in random optical potentials [4].

Numerical studies of wave packet propagation in several models showed that the second moment of the norm or energy distribution grows subdiffusively in time as t^α, with $\alpha \approx 1/3$. Reports on partial localization were published as well [7,8]. Further numerical conductivity studies report Ohmic behavior at finite energy densities [9].

The aim of the present work is to clarify the mechanisms of wave packet spreading and localization. We study two models. First, the Hamiltonian of the disordered discrete nonlinear Schrödinger (DNLS) model:

$$\mathcal{H}_D = \sum_l \epsilon_l |\psi_l|^2 + \frac{\beta}{2} |\psi_l|^4 - (\psi_{l+1}\psi_l^\star + \text{c.c.}) \quad (1)$$

with complex variables ψ_l. The random on-site energies ϵ_l are chosen uniformly from the interval $[-\frac{W}{2}, \frac{W}{2}]$. The equations of motion are generated by $\dot{\psi}_l = \partial \mathcal{H}_D / \partial(i\psi_l^\star)$.

Second, the Hamiltonian of the quartic Klein-Gordon (KG) chain of coupled anharmonic oscillators with coordinates u_l and momenta p_l:

$$\mathcal{H}_K = \sum_l \frac{p_l^2}{2} + \frac{\tilde{\epsilon}_l}{2} u_l^2 + \frac{1}{4} u_l^4 + \frac{1}{2W}(u_{l+1} - u_l)^2. \quad (2)$$

The equations of motion are $\ddot{u}_l = -\partial \mathcal{H}_K / \partial u_l$, and $\tilde{\epsilon}_l$ are chosen uniformly from the interval $[\frac{1}{2}, \frac{3}{2}]$.

We consider a wave packet at $t = 0$ which is given by a single site excitation $\Psi_l = \delta_{l,l_0}$ with $\epsilon_{l_0} = 0$ for the DNLS model, and $x_l = X\delta_{l,l_0}$ with $p_l = 0$ and $\tilde{\epsilon}_{l_0} = 1$ for the KG

chains. The value of X controls the energy E in the latter case.

We will use the DNLS model for theoretical considerations and present numerical results for both models [10]. For $\beta = 0$, Eq. (1) is reduced to the linear eigenvalue problem $\lambda A_l = \epsilon_l A_l - (A_{l+1} + A_{l-1})$. The eigenvectors $A_{\nu,l}$ are the NMs, and the eigenvalues λ_ν are the frequencies of the NMs.

The width of the spectrum $\{\lambda_\nu\}$ is $\Delta = W + 4$. The asymptotic spatial decay of an eigenvector is given by $A_{\nu,l} \sim e^{-l/\xi}$, where $\xi(\lambda_\nu) \leq \xi(0) \approx 100/W^2$ is the localization length [12]. The NM participation number $P_\nu = 1/\sum_l A_{\nu,l}^4$ characterizes the spatial extend (localization volume) of the NM. It is distributed around the mean value $\overline{P_\nu} \approx 3.6\xi$ with variance $\approx (1.3\xi)^2$ [13]. The average spacing of eigenvalues of NMs within the range of a localization volume is therefore $\overline{\Delta\lambda} \approx \Delta/\overline{P_\nu}$. The two scales $\overline{\Delta\lambda} < \Delta$ determine the packet evolution details in the presence of nonlinearity.

The equations of motion of (1) in normal mode space read

$$i\dot{\phi}_\nu = \lambda_\nu \phi_\nu + \beta \sum_{\nu_1, \nu_2, \nu_3} I_{\nu,\nu_1,\nu_2,\nu_3} \phi_{\nu_1} \phi_{\nu_2}^* \phi_{\nu_3} \quad (3)$$

with the overlap integral

$$I_{\nu,\nu_1,\nu_2,\nu_3} = \sum_l A_{\nu,l} A_{\nu_1,l} A_{\nu_2,l} A_{\nu_3,l}. \quad (4)$$

The variables ϕ_ν determine the complex time-dependent amplitudes of the NMs.

The nonlinear frequency shift at site l_0 is $\delta\lambda \approx \beta$. Then we expect three qualitatively different regimes of spreading: (i) $\beta < \overline{\Delta\lambda}$; (ii) $\overline{\Delta\lambda} < \beta < \Delta$; (iii) $\Delta < \beta$. In case (i) the local frequency shift is less than the average spacing between excited modes. Therefore no initial resonance overlap of them is expected, and the dynamics may (at least for long times) evolve as the one for $\beta = 0$. In case (ii) resonance overlap may happen immediately, and

the packet should evolve differently. For case (iii) the frequency shift exceeds the spectrum width. Therefore some renormalized frequencies of NMs (or sites) may be tuned out of resonance with the NM spectrum, leading to self-trapping. The above definitions are highly qualitative, since localized initial conditions are subject to strong fluctuations. Yet, regime (iii) is also captured by a theorem presented in [7], which proves that for $\beta > \Delta$ the single site excitation cannot uniformly spread over the entire (infinite) lattice for the DNLS case.

We order the NMs in space by increasing the value of the center-of-norm coordinate $X_\nu = \sum_l l A_{\nu,l}^2$. We analyze normalized distributions $z_\nu \geq 0$ using the second moment $m_2 = \sum_\nu (\nu - \bar{\nu})^2 z_\nu$ and the participation number $P = 1/\sum_\nu z_\nu^2$, which measures the number of the strongest excited sites in z_ν. Here $\bar{\nu} = \sum_\nu \nu z_\nu$. For the DNLS model, we follow norm density distributions $z_\nu \equiv |\phi_\nu|^2 / \sum_\nu |\phi_\nu|^2$. For the KG chain, we follow normalized energy density distributions $z_\nu \equiv h_\nu / \sum_\nu h_\nu$ with $h_\nu = \dot{a}_\nu^2 / 2 + \omega_\nu^2 a_\nu^2 / 2$, where a_ν is the amplitude of the νth NM and $\omega_\nu^2 = 1 + (\lambda_\nu + 2)/W$.

We systematically studied the evolution of wave packets for (1) and (2) [14]. The above scenario was observed very clearly. Examples are shown in Fig. 1. Regime (iii) yields self-trapping (see also Figs. 1 and 3 of Ref. [7]); therefore P does not grow significantly, while the second moment $m_2 \sim t^\alpha$ with $\alpha \approx 1/3$ [(r), red curves]. Thus a part of the excitation stays highly localized [7], while another part delocalizes. Note that for large $\beta \gg \Delta$ (or similar energy

for the KG model) almost all the excitation is self-trapped. Regime (ii) yields subdiffusive spreading with $m_2 \sim t^\alpha$ and $P \sim t^{\alpha/2}$ [5] [(g), green curves]. Regime (i) shows Anderson localization up to some time scale τ, which increases with decreasing β. For $t < \tau$ both m_2 and P are not changing. However, for $t > \tau$ a detrapping takes place, and the packet starts to grow with characteristics as in (ii) [(b), blue curves]. Therefore regime (i) is a transient, which ends at some time τ, and after that regime (ii) takes over.

Partial nonlinear localization in regime (iii) is explained by self-trapping [7]. It is due to tuning frequencies of excitations out of resonance with the NM spectrum, takes place irrespective of the presence of disorder, and is related to the presence of exact t-periodic spatially localized states (also coined discrete breathers) for ordered [11] and disordered systems [15] (in the latter case t-quasiperiodic states also exist). These exact solutions act as trapping centers.

Anderson localization on finite times in regime (i) is observed on potentially large time scales τ, and as in (iii), regular states act as trapping centers [15]. For $t > \tau$, the wave packet trajectory finally departs away from the vicinity of regular orbits, and deterministic chaos sets in inside the localization volume, with subsequent spreading.

The subdiffusive spreading takes place in regime (i) for $t > \tau$, in regime (ii), and for a part of the wave packet also in regime (iii). The exponent α does not appear to depend on β. In Fig. 2 we show results for $m_2(t)$ in the respective regime (ii) for different disorder strengths. Again we find no visible dependence of the exponent α on W. Therefore the subdiffusive spreading is rather universal.

Let each NM in the packet after some spreading have norm $|\phi_\nu|^2 \sim n \ll 1$. The packet size is then $1/n \gg \overline{P_\nu}$, and the second moment $m_2 \sim 1/n^2$. We can think of two
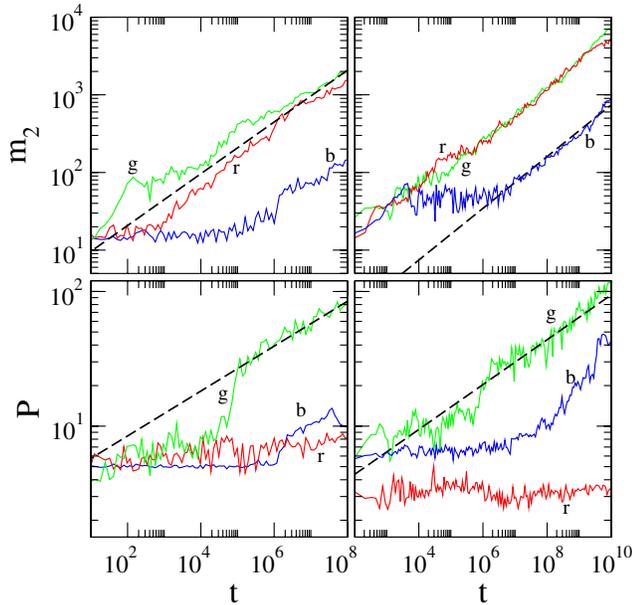

FIG. 1 (color online). m_2 and P vs time in log-log plots. Left plots: The DNLS model with $W = 4$, $\beta = 0.1, 1, 4.5$ [(b), blue; (g), green; (r) red]. Right plots: The KG chain with $W = 4$ and initial energy $E = 0.05, 0.4, 1.5$ [(b), blue; (g), green; (r) red]. The disorder realization is kept unchanged for each of the models. Dashed straight lines are guides to the eye for exponents $1/3$ (m_2) and $1/6$ (P), respectively.
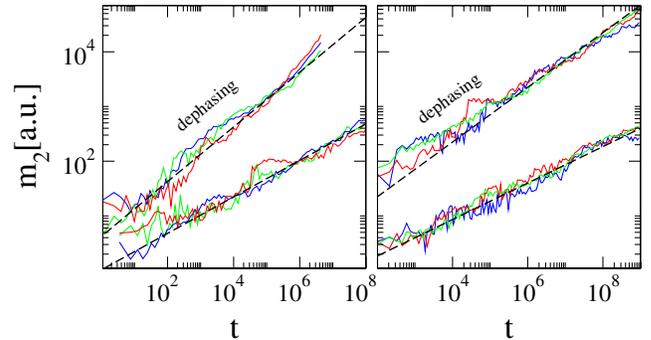

FIG. 2 (color online). m_2 (in arbitrary units) vs time in log-log plots in regime (ii) and different disorder strengths. Lower set of curves: plain integration (without dephasing). Upper set of curves: integration with dephasing of NMs (see text). Dashed straight lines with exponents $1/3$ (no dephasing) and $1/2$ (dephasing) are guides to the eye. Left panel: The DNLS model, $W = 4$, $\beta = 3$ (blue); $W = 7$, $\beta = 4$ (green); $W = 10$, $\beta = 6$ (red). Right panel: The KG chain, $W = 10$, $E = 0.25$ (blue), $W = 7$, $E = 0.3$ (red), $W = 4$, $E = 0.4$ (green). The curves are shifted vertically in order to give maximum overlap within each group.

possible mechanisms of wave packet spreading: a NM with index μ in a layer of width $\overline{P_\nu}$ in the cold exterior, which borders the packet, is either *heated* by the packet or *resonantly excited* by some particular NM from a layer with width $\overline{P_\nu}$ inside the packet. Heating here implies a (sub) diffusive spreading of energy. Note that the numerical results yield subdiffusion, supporting the nonballistic diffusive heating mechanism.

For heating to work, the packet modes should have a continuous frequency part in their temporal spectrum (similar to a white noise), at variance to a pure point spectrum. Therefore at least some NMs of the packet should evolve chaotically in time. Reference [6] assumed that all NMs in the packet are chaotic and that their phases can be assumed to be random. With (3) the heating of the exterior mode should evolve as $i\dot{\phi}_\mu \approx \lambda_\mu \phi_\mu + \beta n^{3/2} f(t)$, where $\langle f(t)f(t')\rangle = \delta(t - t')$ ensures that $f(t)$ has a continuous frequency spectrum. Then the exterior NM is increasing its norm according to $|\phi_\mu|^2 \sim \beta^2 n^3 t$. The momentary diffusion rate of the packet is given by the inverse time it needs to heat the exterior mode up to the packet level: $D = 1/T \sim \beta^2 n^2$. The diffusion equation $m_2 \sim Dt$ yields $m_2 \sim \beta t^{1/2}$ [16]. We tested the above conclusions by enforcing decoherence of NM phases [17] and obtain $m_2 \sim t^{1/2}$ (see Fig. 2). Therefore, when the NMs dephase completely, the exponent $\tilde{\alpha} = 1/2$, *contradicting* numerical observations *without dephasing*. Thus, not all NMs in the packet are chaotic, and dephasing is at best a partial outcome.

Chaos is a combined result of resonances and nonintegrability. Let us estimate the number of resonant modes in the packet. A NM with $|\phi_\nu|^2 = n$ will excite other modes in first order in βn as

$$|\phi_\mu| = \beta n R_{\nu,\mu}^{-1}|\phi_\nu|, \qquad R_{\nu,\mu} \sim \left|\frac{\lambda_\nu - \lambda_\mu}{I_{\mu,\nu,\nu,\nu}}\right|. \qquad (5)$$

The perturbation approach breaks down, and resonances set in, when $R_{\nu,\mu} < \beta n$. We perform a statistical numerical analysis. For a given NM ν we obtain $R_{\nu,\mu_0} = \min_{\mu \neq \nu} R_{\nu,\mu}$. Collecting R_{ν,μ_0} for many ν and many disorder realizations, we find the probability density distribution $\mathcal{W}(R_{\nu,\mu_0})$ (Fig. 3, left plot). The main result is that $\mathcal{W}(x \to 0) \to$ const $\neq 0$. Therefore the probability for a mode in the packet to be resonant is proportional to βn. On average the number of resonant modes in the packet is constant and proportional to β, and their fraction within the packet is $\sim \beta n$. Since packet mode amplitudes fluctuate in general, averaging is meant both over the packet and over suitably long time windows (yet short compared to the momentary inverse packet growth rate). We conclude that the continuous frequency part of the dynamics of a packet mode is scaled down by βn, compared to the case when all NMs would be chaotic. Then the exterior NM is heated according to $i\dot{\phi}_\mu \approx \lambda_\mu \phi_\mu + \beta^2 n^{5/2} f(t)$. It follows that $|\phi_\mu|^2 \sim \beta^4 n^5 t$ and that the rate $D = 1/T \sim \beta^4 n^4$. The
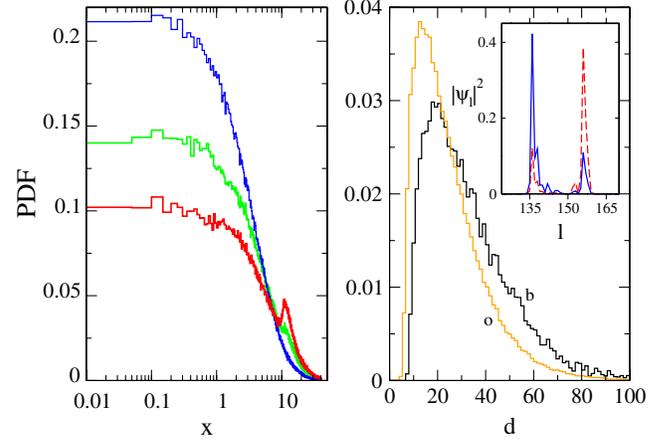

FIG. 3 (color online). Left plot: Probability densities $\mathcal{W}(x)$ of NMs being resonant (see text for details). $W = 4, 7, 10$ (from top to bottom). Right plot: Probability densities $\mathcal{P}(d)$ of peak distances between resonant NM pairs for $W = 4$; (o) orange, $x_c = 0.1$; (b) black, $x_c = 0.01$ (see text for details). Inset: The eigenvectors of a resonant pair of double-peaked states (solid and dashed lines).

diffusion equation $m_2 \sim Dt$ yields

$$m_2 \sim \beta^{4/3} t^\alpha, \qquad \alpha = 1/3. \qquad (6)$$

The predicted exponent is close to the numerically observed one.

In order to clarify the nature of resonant mode pairs, we studied statistical properties of resonant pairs for $W = 4$ with $R_{\nu,\mu_0} < x_c$. Here $x_c \sim \beta n$ is a cutoff value, which decreases the more the packet spreads (in our simulations we reach values $x_c \sim 0.01$). The corresponding distributions of the overlap integral $|I_{\mu_0,\nu,\nu,\nu}|$ appear to be invariant, with an average value $\bar{I} \approx 0.05$. At the same time, the distributions of the frequency spacing $\delta = |\lambda_\nu - \lambda_{\mu_0}|$ favor smaller values the smaller x_c is, with an average spacing $\bar{\delta} = 0.0026$ ($x_c = 0.1$) and $\bar{\delta} = 0.000\,26$ ($x_c = 0.01$). Both NMs from a resonant pair with small R_{ν,μ_0} have a multipeak, or hybrid, structure (inset in Fig. 3, right plot). We evaluated the probability density $\mathcal{P}(d)$ of the peak distance d, estimated with twice the square root of the second moment of the distribution $z_l = A_{\nu,l}^2 A_{\mu_0,l}^2$ (Fig. 3, right plot). Its average increases from $\bar{d} = 24.8$ for $x_c = 0.1$ to $\bar{d} = 32.3$ for $x_c = 0.01$. With the help of semiclassical tunneling rate estimates [18] the level splitting of such a hybrid pair can be estimated to be $\delta \sim A_{\nu,l_0}^2$, where l_0 marks the midpoint between the peaks. This leads to a splitting of the order of $\delta \sim e^{-d/\xi}$. Therefore, an increase of the packet size goes along with a much weaker increase of the distance d, in accord with our above explanation.

Finally we consider the process of resonant excitation of an exterior mode by a mode from the packet. The number of packet modes in a layer of the width of the localization volume at the edge, which are resonant with a cold exterior mode, will be proportional to βn. After long enough spreading, $\beta n \ll 1$. On average there will be no mode

inside the packet, which could efficiently resonate with an exterior mode. Therefore, resonant growth can be excluded.

The subdiffusive spreading is universal; i.e., the exponent α is independent of β and W, which are only affecting the prefactor in (6). Excluding self-trapping, any nonzero nonlinearity strength β will completely delocalize the wave packet and destroy Anderson localization. The exponent α is determined solely by the degree of nonlinearity, which defines the type of overlap integral to be considered in (5), and by the stiffness of the spectrum $\{\lambda_\nu\}$. We performed fittings by analyzing 20 runs in regime (ii) with different disorder realizations. For each realization we fitted the exponent α, and then averaged over all computational measurements. We find $\alpha = 0.33 \pm 0.02$ for the DNLS model and $\alpha = 0.33 \pm 0.05$ for the KG chain. Therefore, the predicted universal exponent $\alpha = 1/3$ explains all available data.

Using the above approach, we estimate the growth of the second moment of a wave packet which is excited on top of a nonzero norm density background n_0. Assuming the wave packet having norm density $(n + n_0)$, we find the rate $D \sim \beta^4 (n + n_0)^4$ and therefore the second moment of the wave packet $m_2 \sim 1/n^2 \sim \beta^4 (n + n_0)^4 t$. It follows that, as long as $n \gg n_0$ holds, the wave packet spreads subdiffusively $m_2 \sim \beta^{4/3} t^{1/3}$. But once the wave packet decays such that $n \sim n_0$, normal diffusion $m_2 \sim \beta^4 n_0^4 t$ sets in, in accordance with [9]. The crossover time scales to infinity as n_0 is approaching zero.

Let us generalize our results to d-dimensional lattices with nonlinearity order $\sigma > 0$:

$$i\dot{\psi}_l = \epsilon_l \psi_l + \beta |\psi_l|^\sigma \psi_l - \sum_{m \in D(l)} \psi_m. \qquad (7)$$

Here l denotes a d-dimensional lattice vector with integer components, and $m \in D(l)$ defines its set of nearest neighbor lattice sites. We assume that (a) all NMs are spatially localized (which can be obtained for strong enough disorder W), and (b) the property $\mathcal{W}(x \to 0) \to \text{const} \neq 0$ holds. A wave packet with average norm n per excited mode has a second moment $m_2 \sim 1/n^{2/d}$. It follows that [19]

$$m_2 \sim (\beta^4 t)^\alpha, \qquad \alpha = \frac{2}{2 + d(\sigma + 2)}. \qquad (8)$$

The exponent α is bounded from above by $\alpha_{\max} = 1/2$, which is obtained for $d = 1$ and $\sigma \to 0$. For the above studied two-body interaction $\sigma = 2$, we predict $\alpha(d = 2) = 1/5$ and $\alpha(d = 3) = 1/7$.

It is a challenging task to determine the bounds of the domains of validity of (8). They will be reached when $\mathcal{W}(x \to 0) \to 0$. Is further growth prohibited then? We think not, because trapping an excitation in a finite volume must generically lead to equipartition on finite times due to nonintegrability. That induces a finite (however weak) chaotic component in the dynamics, which will heat the cold exterior. Extending the above resonance scenario,

higher order resonances are expected to persist and to yield further (though slower) spreading.

[1] P. W. Anderson, Phys. Rev. **109**, 1492 (1958).

[2] S. A. Gredeskul and Yu. S. Kivshar, Phys. Rep. **216**, 1 (1992).

[3] T. Schwartz *et al.*, Nature (London) **446**, 52 (2007); Y. Lahini *et al.*, Phys. Rev. Lett. **100**, 013906 (2008).

[4] D. Clementi *et al.*, New J. Phys. **8**, 165 (2006); L. Sanches-Palencia *et al.*, Phys. Rev. Lett. **98**, 210401 (2007).

[5] D. L. Shepelyansky, Phys. Rev. Lett. **70**, 1787 (1993); M. I. Molina, Phys. Rev. B **58**, 12 547 (1998).

[6] A. S. Pikovsky and D. L. Shepelyansky, Phys. Rev. Lett. **100**, 094101 (2008); I. Garcia-Mata and D. L. Shepelyansky, arXiv:0805.0539v1.

[7] G. Kopidakis *et al.*, Phys. Rev. Lett. **100**, 084103 (2008).

[8] B. Shapiro, Phys. Rev. Lett. **99**, 060602 (2007); S. E. Skipetrov *et al.*, Phys. Rev. Lett. **100**, 165301 (2008).

[9] T. Paul *et al.*, Phys. Rev. A **72**, 063621 (2005); A. Dhar and J. L. Lebowitz, Phys. Rev. Lett. **100**, 134301 (2008).

[10] For small amplitudes the equations of motion of the KG chain can be approximately mapped onto a corresponding DNLS model (see [11] and references therein). In our notations, the norm density of the DNLS model corresponds to the normalized energy density of the KG model and $\beta \approx 3WE$.

[11] R. S. MacKay and S. Aubry, Nonlinearity **7**, 1623 (1994); S. Flach and C. R. Willis, Phys. Rep. **295**, 181 (1998).

[12] B. Kramer and A. MacKinnon, Rep. Prog. Phys. **56**, 1469 (1993).

[13] A. D. Mirlin, Phys. Rep. **326**, 259 (2000).

[14] The system size was typically $N = 1000$ or larger. Excitations did not reach the boundaries during the integration time, and results are unchanged when further increasing N. Symplectic integrators were used for both models to have boundness of the errors. We also varied time step sizes to ensure that results are not influenced by round-off errors.

[15] C. Albanese and J. Fröhlich, Commun. Math. Phys. **138**, 193 (1991); G. Kopidakis and S. Aubry, Phys. Rev. Lett. **84**, 3236 (2000); Physica (Amsterdam) **130D**, 155 (1999); **139D**, 247 (2000); J. Bourgain and W.-M. Wang, J. Eur. Math. Soc. **10**, 1 (2008).

[16] Argumentations in [6] yield an incorrect exponent $\alpha = 2/5$, because the heating rate of the cold exterior was assumed to be equal to the packet diffusion rate, which it is not.

[17] Each 100th time unit with an average of 50% of the NM was randomly chosen, and its phase was shifted by π (DNLS). For the KG case we changed the signs of the corresponding NM momenta.

[18] L. D. Landau and E. M. Lifshitz, *Quantum Mechanics* (Pergamon Press, Oxford, 1977), Sec. 50, task 3.

[19] Dephasing of NMs yields $\tilde{\alpha} = 2/(2 + d\sigma)$.